

Site-selected O 2*p* densities of states in NaV₂O₅ determined from angular-dependent x-ray absorption and emission spectra

G. T. Woods

Department of Physics and Astronomy, The University of Tennessee, Knoxville, Tennessee 37996-1200

G. P. Zhang

Department of Physics and Astronomy, The University of Tennessee, Knoxville, Tennessee 37996-1200 and Department of Physics, State University of New York, College at Buffalo, Buffalo, New York 14222

T. A. Callcott, L. Lin, and G. S. Chang

Department of Physics and Astronomy, The University of Tennessee, Knoxville, Tennessee 37996-1200

B. Sales

Oak Ridge National Laboratory, Oak Ridge, Tennessee 37831

D. Mandrus and J. He

Department of Physics and Astronomy, University of Tennessee, Knoxville, Tennessee 37996-1200 and Oak Ridge National Laboratory, Oak Ridge, Tennessee 37831-6393

(Received 12 June 2001; published 5 April 2002)

We present angular-dependent soft x-ray absorption and emission spectra for the highly anisotropic material NaV₂O₅, which contains three inequivalent oxygen sites located around the V atoms. The polarization direction of the incident photon beam was varied with respect to the crystal axes to obtain strong angular dependence in both the absorption and emission data. Using both energy and angular selection, we obtain local partial densities of states information for each oxygen site, which are compared directly with theoretical results. This technique should be very useful in studies of asymmetric materials such as high-*T_c* superconducting materials with in-plane and out-of-plane oxygen sites.

DOI: 10.1103/PhysRevB.65.165108

PACS number(s): 78.70.En, 78.70.Dm, 71.27.+a

I. INTRODUCTION

Transition-metal oxides have been widely studied within the past few decades for their fascinating magnetic and electronic properties, which include giant magnetoresistance and high-*T_c* superconductivity. As a further example, NaV₂O₅ has attracted recent attention primarily because of a spin Peierls (SP)-like phase transition below 35 K.¹ Subsequent studies have shown that the phase transition involves charge and orbital ordering effects as well as SP dimerization.² Angle resolved photoemission spectroscopy (ARPES) measured the experimental binding energy of the lower Hubbard band derived from V-3*d_{xy}* orbitals.³ The absence of spectral weight at the Fermi level suggests that the system is a Mott insulator, in which strong correlation effects are responsible for its insulating nature. This result has been strongly confirmed by our recent resonant inelastic scattering measurements at the V-*L₃* edge, which demonstrate that correlation splits the V-3*d_{xy}* band that spans the Fermi level.⁴ The ARPES measurements on NaV₂O₅ also show the anisotropic nature of the O-2*p* states in the form of band dispersion. Band structure calculations implementing explicit V-O and V-V hopping integrals provides a useful description of the dispersion associated with the V-3*d_{xy}* orbitals.⁵ The calculation also demonstrated that *p-d* hybridization is an important aspect of the charge-ordered phase of NaV₂O₅, due to its direct effect on the V⁴⁺ *d_{xy}* band dispersion.

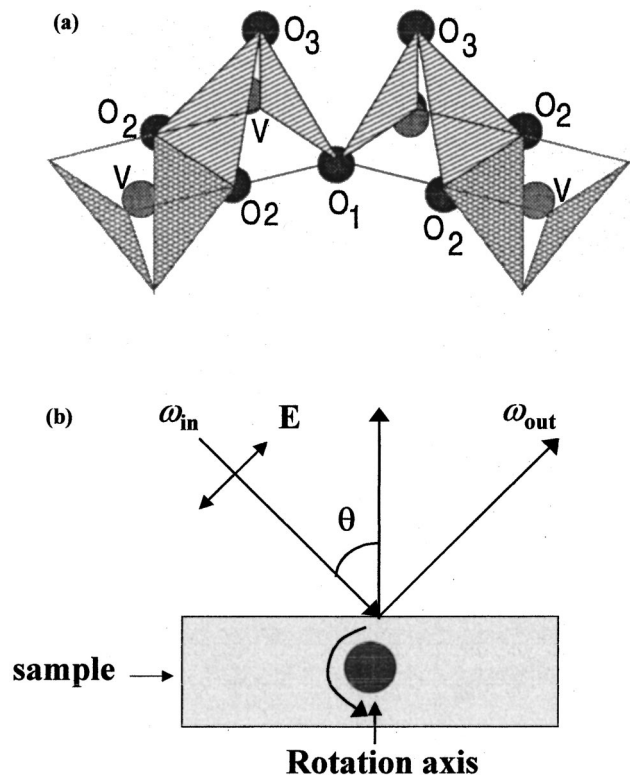


FIG. 1. (a) The structure of NaV₂O₅. (b) The experimental geometry of the sample relative to the polarization vector.

NaV_2O_5 is a highly anisotropic compound, which has a primitive orthorhombic lattice with lattice constants $a = 11.316 \text{ \AA}$, $b = 3.611 \text{ \AA}$, and $c = 4.797 \text{ \AA}$ in the room temperature phase.⁶ The structure of NaV_2O_5 is shown in Fig. 1(a). V_2O_5 forms pyramids, with V inside the pyramid and O sites on the four corners of the basal plane and at the apex. There are three inequivalent O sites and one equivalent V site. Double chains of pyramids extend along the b axis, with the double chains located alternately above and below the a - b plane containing the O1 and O2 oxygen sites. O1 atoms bridge V-O-V rungs of the ladder along the a axis. O2 atoms bridge V atoms along the legs of the ladder and between V atoms in the up and down pyramid chains. O3 atoms are located approximately along the c direction from the V sites and form the apex of the pyramids. The pyramids are slightly tilted and distorted so that the O2 and O3 atoms are shifted slightly away from the b and c axes. There is one equivalent vanadium site with nominal $\text{V}^{4.5+}$ valency. The Na atom donates one extra electron to the structure that is shared between the two V atoms, partially filling a band derived from V d_{xy} orbitals.

There are many advantages of synchrotron based soft x-ray emission (SXE) and absorption (SXA) measurements for the study of anisotropic single crystals of complex compounds. Third generation synchrotron radiation provides the necessary high photon flux, high resolution, and high degree of polarization required for the measurements. Because of the relatively large absorption and emission depths for x rays, the SXE measurements are not surface sensitive. Due to the different binding energies associated with core levels of different elements, SXA and SXE are chemically selective. Since optical transitions obey dipole selection rules, the spectra are also selective for angular momentum state. Thus, measurements at the O- K edge provide LPDOS information on the O- $2p$ states for both the occupied and unoccupied levels.

Studies using linearly polarized x rays have been particularly important in studies of adsorbed molecules on ordered substrates where the molecular bonds have well defined directions. Photoemission studies of CO adsorbed on Ni showed that, with the molecular axis orientated perpendicular to the surface, the π orbitals of the CO were selectively excited when the electric field vector of the photon beam was parallel to the surface.⁷ The principle behind the selective excitations in CO are well understood. When the polarization vector \mathbf{E} is along the molecular axis of the CO molecule, only states with σ symmetry are excited. Thus, the states with π symmetry have zero amplitude. With \mathbf{E} perpendicular to the molecular axis, π symmetry states are detected.⁹ Soft x-ray emission studies of CO on Ni have demonstrated that information on the orientation of molecular orbitals and site selective density of states information is available by rotating the emission spectrometer around the exciting photon beam.⁸ In general, for noncubic single crystals, it is possible to utilize linearly polarized light to selectively excite orbitals with a particular symmetry.¹⁰ For cubic systems, the a , b , and c crystalline directions are equivalent so that polarization effects are not detected.

In this paper, and in a companion theoretical paper¹¹ we

show that important information about bonding angles and site-selected density of states can be obtained in solids for asymmetric crystals, where the distinct sites are located in different crystalline directions. In particular, we present angular dependent SXE and SXA measurements of the highly anisotropic system NaV_2O_5 , at the O- K ($1s$) edge using linearly polarized light. The crystalline axes of the sample are rotated with respect to the fixed directions of the polarization direction of the incident light and the direction of the emitted radiation. We consider both the angular and excitation energy dependence of the O sites and determine the p -like density of states for each. To interpret the data, we calculate element and angular momentum resolved local partial density of states (LPDOS) for the O- $2p$ states at each site. In addition to the band structure calculations, we use the theoretical calculations of angular dependent absorption spectra presented in a companion paper¹¹ to aid in the understanding of the experimental results. Polarization dependent absorption measurements have been carried out on other vanadium oxide materials but have not been analyzed to obtain site selected emission spectra.¹²⁻¹⁴

In NaV_2O_5 , the bonding/antibonding orbitals for each inequivalent oxygen have fixed orientations with respect to the crystalline axes. By aligning \mathbf{E} of our photon beam, we selectively excite the different oxygen sites and obtain site-selected, densities of states information for the $2p$ orbitals. In the measurements reported here, we vary \mathbf{E} in the $a(b)$ - c plane for angles of 15° to 75° measured from the $a(b)$ axis. We have also had some success in obtaining not only selectivity of the oxygen site, but of selected orbitals on a particular site. In particular, the data will show that when we excite into an unoccupied O1- $p\pi$ orbital oriented in the b direction of the crystal, the core hole is refilled from the O1- $p\sigma$ bonding orbitals oriented along the a axis.

II. EXPERIMENTAL PROCESS

The experiments were carried out at beamline 8.0 of the Advanced Light Source at the Lawrence Berkeley National Laboratory. Monochromatized light from the undulator is incident on samples placed within a few mm of the entrance slit of an emission spectrometer.¹⁵ The emission direction is 90° from the incident beam. Incident light is p polarized with respect to the optical plane defined by the incident and emitted photons. To change the angle of incidence of the light (and the polarization direction), the sample was rotated so that its normal was rotated in the optical plane. The emission spectrometer is a Rowland circle design whose measuring efficiency is greatly enhanced through use of a photon-counting area detector which images the full spectrum of interest. Resolving powers to 10 000 are provided by the monochromator and to about 3000 by the emission spectrometer. For the experiments reported here, slits were adjusted to $30 \mu\text{m}$ on the monochromator and $50 \mu\text{m}$ on the spectrometer to provide a resolution of 0.3 eV in the absorption spectra and 0.6 eV in the emission spectra at the O- K edge. Experiments were carried out at vacuums better than 5×10^{-9} Torr. A gold-coated screen was used to monitor I_0 , the incident beam intensity. Total electron yields (TEY),

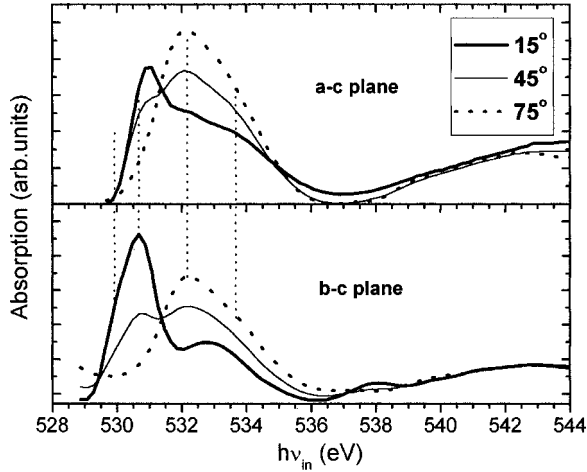


FIG. 2. SXA (TEY) experimental spectra at different angles of incidence. The upper panel scans the a - c plane, while the lower panel scans the b - c plane. Dashed lines locate major spectral features.

which will be the absorption measurements presented in this work, were measured as the ratio of the electron current from the sample to I_0 . The SXE spectra were normalized to the O- K fluorescent yields (not presented). Finally, calibrations of the monochromator and spectrometer energies were done using TiO_2 .

The single crystals of NaV_2O_5 were prepared at the Oak Ridge National Laboratory. NaVO_3 was first prepared by heating Na_2CO_3 (0.99997) and V_2O_5 (0.99995) in a platinum crucible for 2 h at 800 °C. Further VO_2 (0.99) was added and the sample was further annealed and subsequently cooled in a sealed silica ampoule to form samples of NaV_2O_5 in a flux of NaVO_3 . After dissolving the flux with hot water, elongate platelets of approximate dimensions of 1 mm \times 5 mm \times 0.5 mm were obtained. The samples were characterized by x-ray diffraction, specific heat and magnetic susceptibility measurements. The samples were easily cleaved along the c direction to provide clean and flat $[001]$ surfaces containing the a and b axes. It was found that the long dimension was along the b direction and the shorter dimension along the a direction.

III. RESULTS AND DISCUSSIONS

SXA spectra at the O- K edge, as measured by TEY data, are shown in Fig. 2. The spectra are derived from O $1s \rightarrow \text{O } 2p$ transitions. SXA spectra were measured at 7.5° intervals for \mathbf{E} vectors in the a - c (upper panel) and b - c (lower panel) planes. For this report, we present the data taken at 15° , 45° , and 75° , for both crystal orientations with quoted angles measured from the $a(b)$ axis [see Fig. 1(b)]. Each spectrum was taken at 0.2 eV intervals with a collection time of about four seconds per interval. We also note that the axes for the p symmetries in this work refer to the local x , y , and z basis set. For NaV_2O_5 , these symmetries are in the direction of the crystalline a , b , and c axes respectively. In addition, when excitations are such that the polarization vector \mathbf{E} is at an angle of 15° with respect to the $a(b)$ axis in the

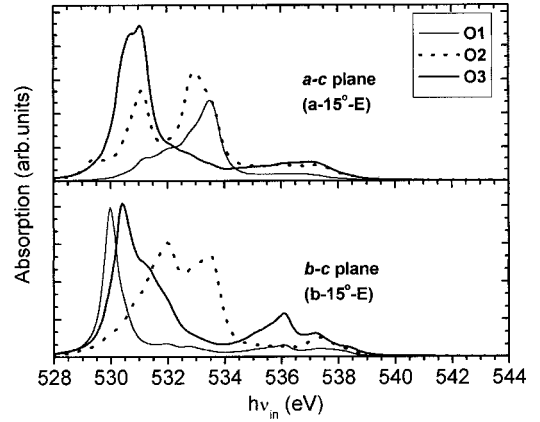


FIG. 3. Theoretical absorption spectra at 15° with respect to the polarization vector of both the a and b crystal axes in the a - c and b - c planes.

$a(b)$ - c plane, we denote this as the a - 15° - \mathbf{E} (b - 15° - \mathbf{E}) configuration. The same notation applies to other angles as well.

In Fig. 2, we see a strong change in the absorption spectra when \mathbf{E} is rotated from a or $b \rightarrow c$. Both sets of spectra show a very strong initial peak for small angles, which drops dramatically as the angle increases. Careful examination reveals, however, that the threshold for b - 15° - \mathbf{E} is almost 1 eV lower than the threshold for a - 15° - \mathbf{E} . Similarly, the initial peak for b - 15° - \mathbf{E} is centered at 530.6, while the initial peak for a - 15° - \mathbf{E} is at 531.2 eV.

Figure 3 displays calculated site-selected absorption curves excited at 15° from the a (a - 15° - \mathbf{E}) and b (b - 15° - \mathbf{E}) axes respectively.¹¹ The energy scale is set by setting the peak for the O3 curve in the b - c plane at 530.5 eV. A comparison of the experimental and theoretical curves clearly shows that the lower threshold for b - 15° - \mathbf{E} is associated with excitation into the O1 site which makes no contribution to the a - 15° - \mathbf{E} curve. A comparison of experimental and theoretical curves permits us to select angle and excitation energies that will selectively excite a single oxygen site. The spectrum characterizing O1 is taken with b - 15° - \mathbf{E} at 529.0 eV, O2 with b - 15° - \mathbf{E} at 533.5 eV and O3 with b - 15° - \mathbf{E} at 530.5 eV and with a - 15° - \mathbf{E} at 529.9 eV. These excitation conditions are further discussed later (see Fig. 6).

Using angular spectra, we can not only excite a particular O site, but also excite orbitals of a particular symmetry. Considering the results from theoretical absorption curves and DOS calculations resolved along the crystalline axes (see Fig. 7), we can say that the low energy of b - 15° - \mathbf{E} is derived mostly from O1- $2p_y$ (π^*) orbitals, which are strongly antibonding with V- d_{xy} orbitals of the V-O1-V rung (see peak A in Fig. 7). In fact, the V- d_{xy} /O1- $2p_y$ coupling strength is due to the tilt of the d_{xy} orbitals around the b -axis and indicates coupling of the $pd \pi$ type.⁶ Thus, the O1- $2p_y$ unoccupied orbitals are emphasized when excitations are along the b axis, perpendicular to both the a and c axes. The remainder of the low energy peak for b - 15° - \mathbf{E} is derived from mainly O3- $2p_y$ orbitals, which are emphasized due to the polarization aligned in the plane of the pyramid. As the case with the O1- $2p_y$ orbitals, they do not contribute to the spectra when

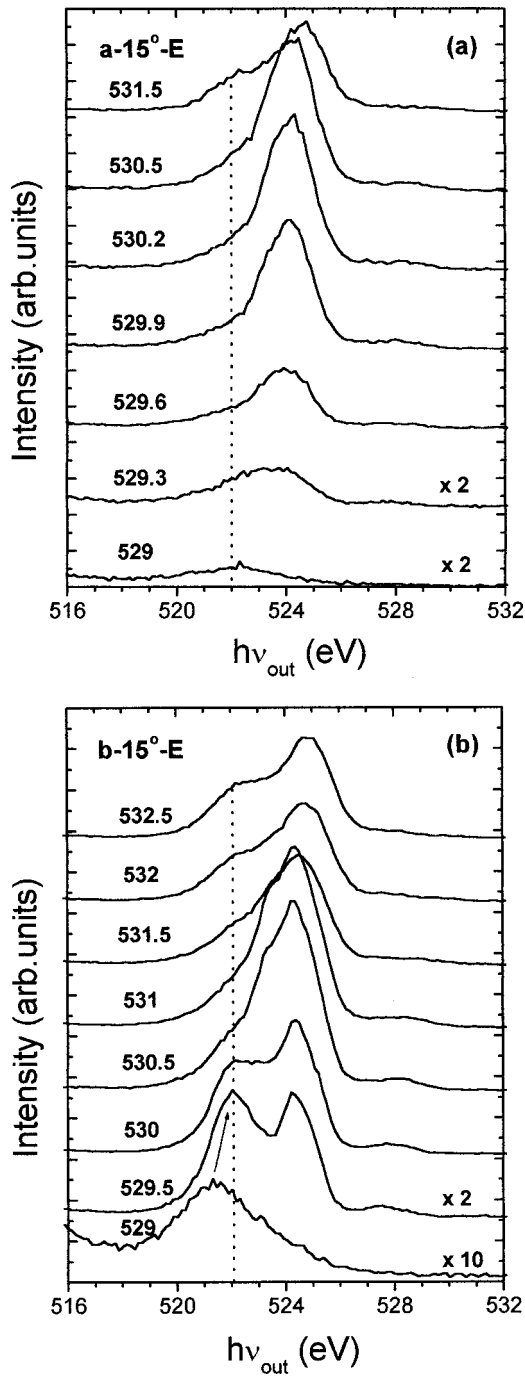


FIG. 4. Experimental emission spectra, as a function of incident photon energy obtained from the absorption curves (see Fig. 2), with the polarization vector \mathbf{E} at 15° with respect to the (a) b axis and (b) a axis.

\mathbf{E} is rotated out of the plane, at which point we see the evolution of the resonance at position 532.3 eV (for both crystal orientations). This resonance is derived from all three O sites.¹¹

Fluorescence spectra were taken at 15° , 45° , and 75° at excitation energies from 529 to 540 eV. In Figs. 4(a) and 4(b), we present fluorescence spectra in the threshold region for the a - 15° - \mathbf{E} and b - 15° - \mathbf{E} excitation conditions, respectively. For the b - 15° - \mathbf{E} excitation, two peaks are observed, a

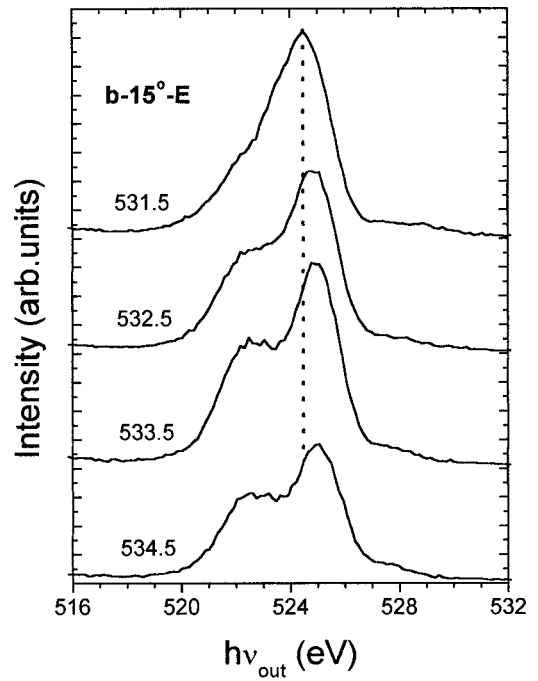


FIG. 5. Emission spectra obtained with excitation energies above the O1 and O3 thresholds. The spectrum taken at an excitation of 533.5 eV represents the LPDOS of the O2- $2p$.

broad low energy peak centered at 522 eV and a structured higher energy peak with a maximum at 524.3 eV. Above an excitation energy of 529 eV, the 524.3 eV peak increases rapidly with energy, reaching a maximum at an excitation energy of 530.5 eV, the maximum of the absorption spectrum. Using the theoretical calculation of Fig. 3 as a guide, we take the spectrum excited at 530.5 eV to be representative of fluorescence from the O3 site. Since the O1 site is not excited at low excitation energies in the a - 15° - \mathbf{E} configuration, another measure of the O3 fluorescence spectra is provided by excitation at 529.9 eV in this configuration.

For the b - 15° - \mathbf{E} excitation condition, the very strong

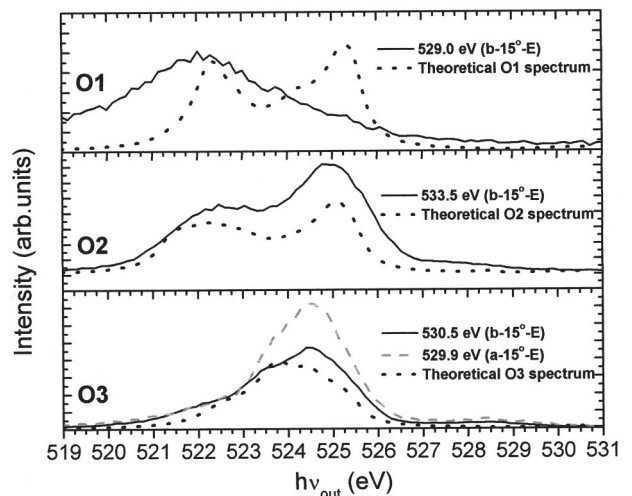


FIG. 6. Experimental (solid) and theoretical (dotted) emission spectra representing the LPDOS of each O site.

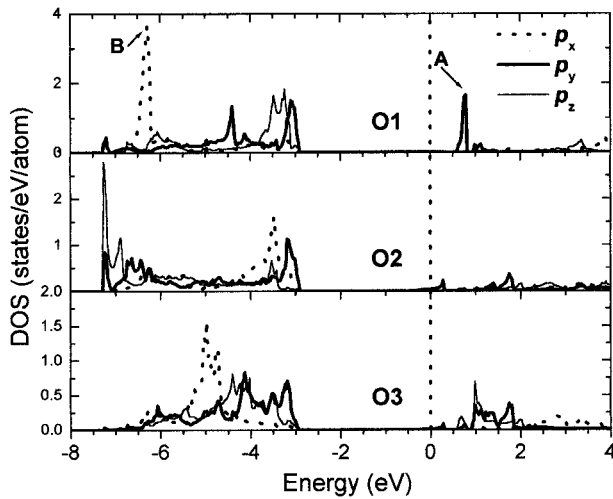


FIG. 7. Projected DOS of the different 2*p* symmetries.

emission from the O3 site, identified from the 524.3 eV peak, decreases at low excitation energies and disappears entirely for an excitation energy of 529 eV. We take the spectrum excited at 529 eV as representative of the O1 spectrum, with the O3 spectrum eliminated. Similar representative O1 spectra may be obtained by scaling and subtracting the 530.5 eV spectrum (representing O3) from the composite O1 plus O3 spectra taken at 529.5 or 530 eV. A close study of the 529 eV spectrum indicates that its maximum is displaced by about 0.5 eV below the comparable peak in the normal fluorescence spectra excited at higher energies. This shift is characteristic of resonant inelastic x-ray spectra that are excited below the normal threshold.^{15–17}

In Fig. 5, we present spectra taken in the b -15°- \mathbf{E} configuration for excitation energies in the region where excitation shifts from the O3 to the O2 site. There are clear changes in the shape, structure and position of the spectral features as excitation changes from 530.5 eV where primarily O3 is excited to 533.5 eV, where O2 is primarily excited. We take the 533.5 eV spectrum as representative of nearly pure O2 excitation.

To illustrate our conclusions, we present a LPDOS plot, both experimental and theoretical, for each O site in Fig. 6. In addition, the O-2*p* DOS's for each site are presented in Fig. 7. Calculations were performed utilizing the WIEN97 computer code.¹⁸ The exchange correlation part of the potential was approximated by the GGA method.¹⁹ The calculation was converged to the total energy with 512 k points in the irreducible wedge. Good agreement is reached with calculations performed using the linearized muffin tin approximation (LMTO) (Ref. 5) and that of the linear combination of atomic orbitals (LCAO).²⁰ Both of these works implemented on-site Coulomb repulsion corrections. However, in both cases, due to the fact that the 2*p* electrons are much less correlated, the O-2*p* DOS was unaffected.

In Fig. 6, we compare the spectra identified in the preceding paragraphs as representative of O1, O2, and O3 excitation with the theoretical site-selected O- K emission spectra calculated with the WIEN97 code. Very good agreement is obtained between experimental and theoretical curves of the

O2 and O3 sites. There is excellent agreement of the location of structural features and moderately good agreement in the relative magnitude of experimental and calculated structural features.

The agreement for the O1 spectrum is much less satisfactory. Only the low energy peak centered at about 522 eV in the theoretical spectrum is observed as a distinct feature of the experimental spectrum. The strong peak located at about 525 eV in the calculated spectrum is observed only as a featureless sloping shoulder in the experimental spectrum.

The implications of this result can be better understood by considering the projections of the O- p density of states of the different p symmetries presented in Fig. 7. The theoretical emission curves in Fig. 6 are calculated as normal fluorescence spectra, which do not consider the polarization of the exciting photons, and give equal weight to the p_x , p_y , and p_z components of the density of states. As noted above, this gives good agreement for the O2 and O3 sites, but not for O1. Figure 6 makes clear that excitation of the O1 site at threshold occurs when the polarization vector of the exciting photons is aligned with O1- $p\pi$ antibonding orbital (p_y projection) directed along the b axis of the crystal. In the emission spectra, the low energy peak, which dominates the spectrum, is associated with the O1- $p\sigma$ bond orbital (p_x projection) between the bridging oxygen and the adjacent vanadium atoms (peak B in Fig. 7). The contributions of the p_y and p_z are strongly suppressed in the experimental spectra.

Though this result is not yet fully understood theoretically, we believe that it is a result of below threshold excitations via the RIXS process, in which electronic excitations between orbitals of different spatial symmetry are suppressed. In hexagonal boron nitride (BN), for example, energy loss to π - π^* transitions is suppressed in the RIXS spectrum, but de-excitations for the π states are readily observed in normal fluorescence spectra.¹⁵

Referring to O2, the very bottom of the band is derived from O2- $2p_z/V$ -4*s* bonding orbitals, while the top of the band is derived from mainly $2p_{x,y}$ orbitals. In addition, to the high energy side of the main O-2*p* band is a small spectral feature, which is seen at low excitation energies, especially along the b -15°- \mathbf{E} configuration. This spectral feature is derived from the weakly bonding V-3*d*/O2- $2p_y$ orbitals, which is due to the slight tilt of the VO₅ pyramids. The spectral intensity is seen tracking somewhat with the excitation energy, which is in part due to the correlation effects (d - d transitions) within the V 3*d* electrons. However, the weak hybridization allows for one to disregard the V-O interactions when accounting for correlation effects of the V-3*d* electrons.⁴ Finally, for the O3 spectra, the theoretical and experimental curves are in agreement with contributions from all three p symmetries. The O3- $2p_x$ orbitals, as is the case with O1- $2p_x$, are bonded with V-3*d* _{x^2-y^2} orbitals.^{5,20}

In summary, we have shown that angular dependent SXA and SXE is an invaluable technique to study the electronic structure of anisotropic systems. We have demonstrated explicitly the effects of p - d hybridization on the O sites, specifically that of the O1- $2p_y$ antibonding orbitals. By scanning the polarization vector in both the a - c and b - c planes,

we were able to measure, to a very good approximation, the LPDOS of the $2p$ orbitals of each inequivalent O site. Good agreement was reached between the band structure calculations and experimental results.

ACKNOWLEDGMENTS

This research was supported by NSF DMR-9801804 and NSF DMR-0072998. Oak Ridge National laboratory is man-

aged by UT-Battelle, LLC, for the U.S. Department of Energy under Contract No. DE-AC05-00OR22725. We would like to thank the staff at the Advanced Light Source, especially Jonathon Denlinger, for their support. Also, we would like to thank Christain Halloy and the rest of the JICS staff for their help with the computations performed on the IBM-SP2 supercomputer.

-
- ¹M. Isobe and Y. Ueda, *J. Phys. Soc. Jpn.* **65**, 1178 (1996).
²M. V. Mostovoy and D. Khomskii, *Solid State Commun.* **113**, 159 (2000).
³K. Kobayashi *et al.*, *Phys. Rev. Lett.* **80**, 3121 (1998).
⁴G. P. Zhang, T. A. Callcott, G. T. Woods, L. Lin, B. Sales, D. Mandrus, and J. He, *Phys. Rev. Lett.* **88**, 077401 (2002).
⁵A. N. Yaresko, V. N. Antonov, H. Eschrig, P. Thalmeier, and P. Fulde, *Phys. Rev. B* **62**, 15 538 (2000).
⁶H. Smolinski, C. Gros, W. Weber, U. Peuchert, G. Roth, M. Weiden, and C. Geibel, *Phys. Rev. Lett.* **80**, 5164 (1998).
⁷R. J. Smith *et al.* *Phys. Rev. Lett.* **37**, 1081 (1976).
⁸A. Nilsson *et al.*, *Phys. Rev. B* **51**, 10 244 (1995).
⁹E. W. Plummer, in *Topics in Applied Physics*, edited by R. Gomer (Springer-Verlag, New York, 1975), Vol. 4.
¹⁰F. Brouder, *J. Phys.: Condens. Matter* **90** (1992).
¹¹G. P. Zhang, T. A. Callcott, G. T. Woods, L. Lin, B. Sales, and D. Mandrus (unpublished).
¹²R. Zimmerman, R. Claessen, F. Reinert, P. Steiner, and S. Huffner, *J. Phys.: Condens. Matter* **10**, 5697 (1998).
¹³F. M. F. de Groot, *J. Electron Spectrosc. Relat. Phenom.* **62**, 111 (1993).
¹⁴S. Gerhold, N. Nücker, C. A. Kuntscher, S. Schuppler, S. Stadler, Y. U. Idzerda, A. V. Prokofiev, F. Büllsfeld, and W. Assmus, *Phys. Rev. B* **63**, 073103 (2001).
¹⁵J. J. Jia, T. A. Callcott, E. L. Shirley, E. A. Hudson, L. J. Terminello, A. Asfaw, D. L. Ederer, F. J. Himpsel, and R. C. Perera, *Phys. Rev. Lett.* **76**, 4054 (1996).
¹⁶L. Duda and J. Downes, *Phys. Rev. B* **61**, 4186 (2000).
¹⁷P. Carra, M. Fabrizio, and B. T. Thole, *Phys. Rev. Lett.* **74**, 3700 (1995).
¹⁸P. Blaha, K. Schwartz, and J. Luitz, WIEN97, A Full Potential Linear Augmented Plane Wave Package for Calculating Crystal Properties (Karlheinz Schwarz Techn. Univ., Wien, Vienna, 1999). ISBN 3-9501031-0-4.
¹⁹J. P. Perdew, S. Burke, and M. Ernzerhof, *Phys. Rev. Lett.* **77**, 3865 (1996).
²⁰H. Wu and Q. Zheng *Phys. Rev. B* **59**, 15 027 (1999).